Chapter

Comparative Analysis Carried Out on Modern Indentation Techniques for the Measurement of Mechanical Properties: A Review

Saquib Rouf, Sobura Altaf, Shezan Malik, Kaleem Ahmad Najar and M.A. Shah

Abstract

Nowadays many indentation techniques are being commonly employed for determining some mechanical properties (harness, elastic modulus, toughness, etc.) using simple method of measuring the indentation depth. On the basis of measurement of depth of penetration, indentation technique has be classified into major categories i.e. microindentation and nanoindentation. Nanoindentation technique uses indirect method of determining the contact area as the depth of penetration is measured in nanometers, while in conventional indentation the area in contact is measured by elementary measurement of the residual area after the indenter is removed from the specimen. Dynamic hardness is the best result of dynamic indentation which can be expressed as the ratio of energy consumed during a rapid indentation to the volume of indentation. The parameter which are taken into consideration are indentation depth, contact force, contact area, mean contact pressure.

Keywords: hardness, elastic modulus, nano/microindentation, Berkovich indenter, spherical indenter & vicker indenter

1. Introduction

We are having distinct techniques to rule out the mechanical properties of materials; one among them is nanoindentation. Nanoindentation is the most accepted method to regulate the mechanical properties like hardness, elastic modulus, toughness and stiffness of a material. Thus, nanoindentation is also noted by its different names in mechanical engineering field like; depth sensing indentation (DSI), instrumental indentation technique (IIT) and universal hardness test (UHT).

The indenter is the main component of nanoindentation testing which is pressured through the exterior of a material. With a prescribed load, the displacement of the indenter inside a material is observed. The hardness of the material is shown by the equation:

$$H = \left(\frac{P_{max}}{A_r}\right)$$

Where, P_{max} is a maximum load for depth (h) and A_r is the residual area or the projection of indenter. This residual area inside a material is then measured by atomic force microscope. The residual area builds upon the kind of indenter and material of indenter. Therefore, the mechanical properties can vary as the penetrating material changes from one experiment to another.

The nanoindentation is also used to measure reduced elastic modulus and the sample modulus by using the following Equations [1];

$$\text{Reduced elastic modulus}, E_r = \frac{dP}{dh} \times 1/2 \times \frac{\sqrt{\pi}}{A_{r.}}$$

$$\text{Sample modulus}, E_s = \left(1 - v_s^2\right)\left(\frac{1}{E_r} - \frac{1 - v_i}{E_i}\right)$$

Where, E_i is the modulus of indenter and, v_s and v_i is the poisson's ratio for sample and indenter, respectively [1, 2].

1.1 Types of indenters

The various types of indenters with their specifications are mentioned in **Table 1** [3]. Generally, nanoindentation itself has a wide range of applications in physical science and concedes us to examine nanoscale surface adjustments in solid materials and specify the appearing variations in its mechanical response. From atomic structure to atomic defects, this has made a revolution in material engineering. It can be used to study discrete atomic rearrangement of specimen under loading conditions. When equipped with Raman spectroscopy and Atomic Force Microscope, it can find its place in studying lattice dislocations [4].

From literature survey, it has been found that results of nanoindentation depend upon the indenter tip, shape and its orientation [5]. AFM plays a vital role in nanoindentation process. It is used to measure the residual indentation area of the specimen which is further used to calculate hardness of material. It has been clearly observed and proved that nanoindentation results depend upon the type of indenter used. So, we can say that nanoindentation results vary for different indenters. To achieve better results in indentation process, continuous nanoindentation has been introduced. This approach involves intially loading the indenter at peak load and then unloading 90% of the peak load for 50 seconds and keeping it after 90% of unloading for almost 100 seconds and lastly unloading wholly the indenter. The continuous nanoindentation is used to find stiffness in terms of indentation depth in a one shot experiment.

Indenter	Projected area	Semi angle
Sphere	$2\pi Rh_p$	Not available
Berkovich	$3h_p^2(\tan\theta)^2$	65.3°
Vickers	$4h_p^2(\tan\theta)^2$	68°
Knoop	$2h_p(\tan\theta_1)(\tan\theta_2)$	$\theta_1 = 86.25°$, $\theta_2 = 65°$
Cube Cone	$3h_p^2(\tan\theta)^2$	35.26°
Cone	$\pi h_p^2(\tan\alpha)^2$	α (effective cone angle)

Table 1.
Indenter specifications [3].

1.1.1 Spherical indenter

Spherical indenters are used for soft materials. It has been established that even a single alteration of the indenter size or radius can give collectible observation into heterogeneous aspects of the radiation-induced-damage region. The most common spherical indenter known is diamond spherical indenter which has radius less than 1 micron. We know that indentation hardness is used as; $H = \frac{P}{A}$, where, P is the applied load and A is the area of indenter.

The indentation hardness equation can be also known as $= \frac{4P}{\pi d^2}$, where, d is the diameter of contact circle when at full load. The nanoindentation deals with the size of impression, whose area is to be calculated and is found by [1–3]:

$$A = 2\pi R_i h_c$$

where, R_i is radius of the indenter and h_c is the depth of contact also called contact depth.

The Brinell hardness number for spherical indenters is calculated as [6]:

$$BHN = \frac{2P}{\pi D(D - \sqrt{D^2 - d^2})}$$

Where, D is the diameter of indenter. The Brinell hardness number depends on the real curved surface response.

Researcher [7] has adopted the use of spherical indenter to figure out the structural characteristics of SS400, SM490 and SM520 using finite element analysis to create a shift of algorithm. The specifications taken under consideration are yield strength (σ_y), the hardening exponent (n), and the ratio (α). The α here is characterized as the ratio between the strain at beginning point of strain hardening and the yield strain. The spherical indenter with the value of 1141GPa as elastic modulus and that of poisson's ratio as 0.07, the radius of the indenter is put up to R = 5 μm and the maximum indentation depth is kept 0.3R, the results derived from the indentation process on the above mentioned specimens are very much reliable with the proposed model of reverse algorithm and can provide the best parameters of structural steel. Thus, the study of the radius of the indenter is an important factor for supposition of disorder nucleation shear stress implied from spherical indentation retortion.

Dynamic indentation of elastic plastic solid has been also reported here [8]. Dynamic hardness is the best result of dynamic indentation which can be expressed as the ratio of energy consumed during a rapid indentation to the volume of indentation. There is a restraination to either the displacement or the force of the indenter by the indentation equipment. Indentation depth, contact area, contact force, and mean contact pressure were the parameters that are taken into account and the finite element technique has been operated to determine the contact issues. The author observed that parameters like contact force, contact area and mean contact pressure are directly dependent on indentation velocity irrespective of material's elastic plastic property. The dynamic indentation of a material is linked to a dimensionless parameter which can be attained as the ratio between the kinetic energy density shifted towards the indented material to the sufficient net energy of the material and the initial yield. It has been seen that this dimensionless parameter is associated with the plastic deformation of a solid which implies larger the dimensionless parameter larger will be the plastic deformation of solid. Down below **Figure 1** distinguishes the types of indenters [9] as: (a) Spherical (b) Conical (c) Square- pyramidal (vicker) & (d) Berkovich, respectively.

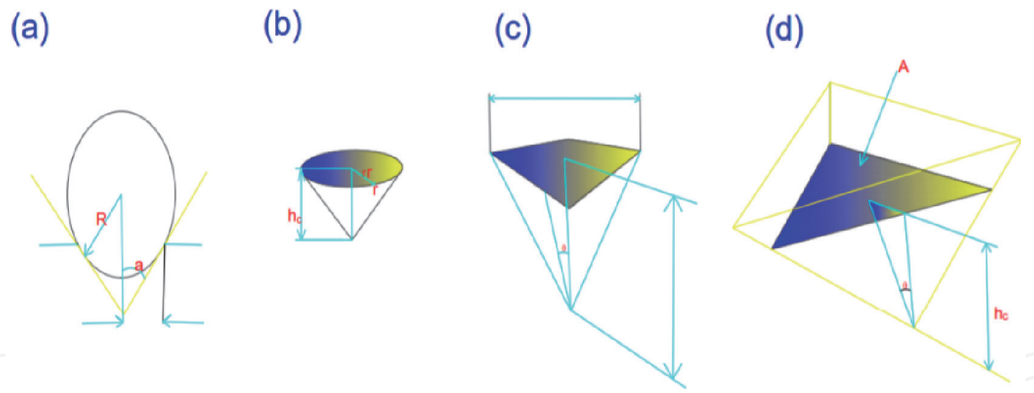

Figure 1.
Types of indenters [9]: (a) spherical (b) conical (c) square- pyramidal (vicker) & (d) Berkovich.

1.2 Berkovich indenter

The Berkovich indenter tip has a geometry of a three-sided pyramid that can be rested to a point, hence upholding a self-similar geometry to very small extent. This geometry is generally much approved than the Vickers indenter tip which has a geometry of four-sided pyramid. It is most often preferred for certaining the mechanical parameters of materials. Berkovich indenter with geometry of three sided pyramid contains a face angle of 65.3° between the sides. The indenter tip is blunted and has been constructed with the hard materials example diamond. It is more precise than vicker indenter due to its sharp point. The Berkovich indenter tip is of optimal use for most testing funtions. It is not easily impaired and can be promptly built. It brings about plasticity at slight loads too generating a relevant share of hardness. The Berkovich indenter tip is feasible as a traceable standard.

On the specimen, the projected area of Berkovich indenter is given as [3]; $A_p = 3\sqrt{3}h_c^2(\tan\theta)^2$, where θ is the face angle. For $\theta = 65.3°$, $A_P = 24.5h_c^2$.

Further, the Meyer hardness is given by [10]:

$$H = \frac{P}{A_P} = \frac{P}{24.5h_c^2}$$

From the above equation we can conclude that Meyer hardness for Berkovich indenter is the function of contact depth. Researchers [11] have reported the nanoindentation of zirconia yttria and alumina zirconi-yttria with the help of the Berkovich diamond indenters having a tip radius of 20 to 25 nm. The main function of this indentation practise is to resolve the mechanical properties like modulus of elasticity (E) and fracture toughness of the above mentioned biomedical ceramics. The values of mechanical properties are calculated at different loads like 1.5 mN, 2 mN and 5 mN. The frequency for indentation is 75 Hz with poisson's coefficient v = 0.25. AFM is engaged in the analysis of the continuing samples of nanoindentation. The equation given below (Sneddon equation) is employed in the calculation of the modulus of elasticity [12]:

$$S = 2\beta\sqrt{\left(\frac{A}{\pi}E_r\right)}$$

Where, A is the area of contact which in return is a function of indentation depth (h) also called as depth of penetration. E_r is reduced modulus of elasticity and β which is a constant based upon the geometry of indenter and for Berkovich

indenter value of β is 1.034. The modulus of elasticity is calculated by the following Equation [13]:

$$E = \frac{1 - V^2}{\frac{1}{E_r} - \frac{1 - V_i^2}{E_i}}$$

Where, E_i, E and V_i, V are constants of modulus of elasticity and poisson's ratio of diamond indenter and specimen respectively. Further fracture toughness of the material is given as [14]:

$$K = k\left(\frac{E}{H}\right)^{\frac{1}{2}}\left(\frac{P}{C^{3/2}}\right)$$

Where, H is the hardness of material, P is the load practiced, E is the modulus of elasticity, k is empirical constant depending upon the geometry of indenter and c is the crack length. The results obtained are mentioned in **Table 2**.

Generally, Chech et al. [15] reported the bluntness of Berkovich indenter in their research. The materials that were employed were those whose young's modulus were already known; like fused silica and BK7 glass. The indentation results were compared with the results from AFM. It was found that the pointless radius of a spherical cap representing the indenter bluntness depends upon the technique accepted.

1.3 Vicker indenter

The Vickers indenter resembles to pyramid of square shape with faces and edges at angles of 68° and 148° respectively. The most common vicker indenter is vicker diamond indenter. The vicker hardness is given as [16]:

$$VH = 1.8544\frac{P}{d^2}$$

Where, d is the distance from one corner to its opposite corner of the projection left on the specimen. The Meyer hardness of vicker indenter is given by [17]:

$$H = \frac{2P}{d^2}$$

Also, the projected area of indenter, $A_p = 4h_c^2(\tan\theta)^2$, where θ is the face angle and is equal to 68°, h_c is the contact depth [18].

Material	Composition	Modulus of Elasticty (GPa)	Nano-hardness (GPa)	Stiffness (N/m)	K_{ic} (Mpa)
ATZ	20wt%Al_2O_3 + 80wt%TZ-3Y	355 ± 7	21 ± 1.2	157,471 ± 12	4.2 ± 0.1
ZTA	80wt%Al_2O_3 + 20wt%TZ-3Y	360 ± 6	35 ± 1	161,190 ± 12	3.50 ± 0.2
3Y-TZP	97%molZrO_2 + 3%molY_2O_3	354 ± 7	25 ± 0.8	83,886 ± 9	5.1 ± 0.2
8Y-CSZ	92%molZrO_2 + 8%molY_2O_3	385 ± 2	31.3 ± 0.2	153,423 ± 12	3.77 ± 0.02

Table 2.
Mechanical properties of various materials [11].

The vicker indenter is utilized in determination of the fracture toughness of brittle materials example glass. Fracture toughness (*KC)* is explained as resistance offered by a material to abrupt generation of cracks [19]. However, Anstis et al. [20] proposed an equation to measure the fracture toughness. This equation was a result of experiments on 16 materials. The equation for fracture toughness is given below:

$$K_{ic} = \chi\sqrt{\frac{E}{VH}}\frac{P}{C^{\frac{3}{2}}}$$

The above equation has an uncertainty of 25%, in this equation, *VH* is the vicker hardness, *E* is the modulus of elasticity in Mpa and χ is the dimensional less constant based upon the frame of indenter and geometry of crack generated. Usually χ varies from 0.016 to 0.004 for vicker indenter.

Herval et al. [21] reported the comparison of fracture toughness from vicker indenter using Anstis equation for these materials; crown glass (BK7), heavy flint glass (SF17), zerodur glass and hydroxyapatite ceramic. The experimentation has been performed on Zwick Roell with load varying from 2 to 100 N with dwell time at maximum load of 10 seconds. The Cracks are examined using optical microscope. Thus, the results obtained are summarized in the **Table 3**. The authors conclude by verifying that fracture toughness remains constant for a specific material under varying loads. This means that polishing does not generate residual stress on sample.

1.3.1 Fracture toughness of Y-TZP dental ceramic

Fracture toughness is the basic criteria for studying the potential of bio ceramics. The most common ceramic used is zirconia. It finds its application in bone and dental implants. Y-TZP dental ceramic contains 2–3 mol% of yttrium oxide which produces of 6MPam1/2 [22]. Donaka [23] reported the indentation of Y-TZP dental ceramic by vicker indenter. The samples were cut into 10 × 10 × 2 mm plates. Following four set of loads were applied; 24.03 N (VH3), 49.03 N (VH5), 196.13 N (VH20) and 294.20 N (VH30). Each load has been applied 30 times. The fracture toughness has been directly determined by crack length. **Table 4** can sum up the above experiment.

The data above shows that with the increase in applied load, the hardness of Y-TZP increases. This reaction is recognized as normal indentation size effect [24]. Fracture toughness depends upon the type of crack formed. So, for the process of attaining the fracture toughness of a material, the fundamental step is to notice the type of crack formed. Usually palmqvist and median cracks are formed due to vicker indentation. Palmqvist cracks can be found in tough materials at high loads and in brittle materials at low loads [25]. Depending upon the type of crack developed various methods have been used to calculate fracture toughness. Some of them are mentioned in the **Table 5**.

The vicker indentation on Y-TZP Ceramic results in crack propagation which is further used to calculate fracture toughness. Crack propagation mainly depends

Parameter	Crown glass	Heavy flint glass	Zerodur glass	Hydroxyapatite ceramic
K_{ic} (MPa)	0.5±0.40	0.47 ± 0.03	0.93 ± 0.1	1.20 ± 0.03
VH (GPa)	6.3 ± 0.3	4.4 ± 0.3	6.7 ± 0.6	4.4 ± 0.6

Table 3.
Comparison of fracture toughness by vicker indenter.

Load	Vicker hardness (average)
VH3	1379
VH5	1344
VH20	1345
VH30	1337

Table 4.
Fracture toughness of Y-TZP with varying loads.

Author	Crack type	Equation
Casellas [26]	Palmqvist	$0.024\frac{F}{C^{3/2}}\left(\frac{F}{VH}\right)^{1/2}$
Palmqvist [27]	Palmqvist	$0.0028VH^{1/2}.\left(\frac{F}{VH}\right)^{1/2}$
Shetty et al. [28]	Palmqvist	$0.0319\frac{F}{al^{1/2}}$
Niihara et al. [29]	Palmqvist	$0.0089\left(\frac{E}{VH}\right)^{2/5}\frac{F}{al^{1/2}}$
Anstis [30]	Median	$0.016\frac{F}{C^{3/2}}\left(\frac{E}{VH}\right)^{1/2}$
Evans and Charles [30]	Median	$0.0752\frac{F}{C^{3/2}}$
Tanaka [30]	Median	$0.0725\frac{F}{C^{3/2}}$
Niihara, Morena and Hasselman [29]	Median	$0.0309\left(\frac{E}{VH}\right)^{2/5}\frac{F}{C^{3/2}}$
Lankford [28]	Anykind	$0.0782(VHa^{1/2})\left(\frac{E}{VH}\right)^{2/5}\left(\frac{C}{a}\right)^{1.56}$

Table 5.
Various methods to calculate fracture toughness depending upon the crack formed [26–30].

upon the indentation load applied and the type of material. For E = 210 GPa, the fracture toughness of palmqvist crack varies from 4.96 to 7.73 MPam1/2 and 3.96 to 6.72 MPam1/2 for median crack profile. The lankford model gives the highest of values 7.73 MPam1/2 for 29.42 N and Anstis give lowest of 4.49MPam1/2 for 294.20 [28–30].

1.4 Nanoindentation for nuclear materials

The nanoindentation technique for irradiated materials started back in 1986 [31]. From last few decades, nanoindentation has been acknowledged as well founded means to explore the bounded mechanical properties at small scale. Therefore, the idea of the sequence of ion irradiation and nanoindentation has been greatly advanced in later years to examine the mechanical role of nuclearly arranged materials with irradiation developed.

Various studies [32–34] have been performed on the different combination of materials with the focus on effect of crystal structure and irradiation temperature on hardness of material. For ion irradiation there is a plan of action that needs to be followed to observe the irradiation damage prompt by energetic neutrons. It is very difficult to evaluate the mechanical properties of ion irradiated materials. The most important factors are limited indentation depths and inhomogenous distribution of irradiation induced defects [35]. Additionally, upon ion-irradiation the metal surface is modified by a thin radiation-damaged layer which causes a change in its mechanical response as compared to the bulk of the sample. In order to successfully study the effects of radiation damage on the indentation behavior, we need to first

decouple the effects of orientation from the effects of the increased defect density caused by irradiation. It was observed that there exists a strong orientation effect of radiation which induces mechanical changes at the grain scale. Obviously, surface energies for the orientation is quite different. So there can be significant differences in the damage experienced by these grains [36, 37].

The impact of high energy particles on the metalic materials for energy systems are widely studied as the mechanical properties of these materials are highly effected [38, 39]. This study is very important to develop a smart and effective nuclear energy production system. Mechanical characterization methods like uniaxial compression and tension remain invalid [40], as high spatial resolution is required [41–43]. Since nanoindentation gives rich statistical data [44, 45], hence it is convenient for mechanical characterization of ion irradiated materials. Nanoindentation for irradiation material can be broadly classified into two categories; suface nanoindendation and cross-sectional nanoindentation [36, 46].

For irradiated materials, spherical indentation is widely preferred over berkovich indentation as it can analyze the irradiation effect not only on materials yielding but also the elasto-plastic transition and strain hardening behavior, by converting the force-depth (F h) relationships into the indentation stress–strain (ISS) relationships [47, 48]. High temperature nanoindentation can be used to determine the thermo-mechanical behavior of irradiated materials at the actual working temperature [49].

1.5 Nanoindentation for polymeric materials

From past one decade, the use of polymeric composite matrix has been widely used due to their high energy absorption, light weight and good adhesion [50]. A large number of researchers [50–53] have reported the nanoindentation on polymeric surfaces and it has been observed that assessment of elastic modulus has remained a challenge. For nanoindentation of soft polymeric materials, the materials complaince can create difficulties in tracing the initial contact [54]. Researcher [55] has shown the main problem of nanoindentation with polymeric materials, the elastic moduli obtained by nanoindentation does not coincide with the moduli obatined by conventional micro tension and compression. There has been an increase in the moduli obtained by the nanoindentation of polymeric materials. Studies performed on polystyrene and polycarbonate show 64% and 70% shift in moduli, respectively [52]. Moreover, for PMMA [56], 67% shift is seen and 20% for poly bemzocyclobutene [53]. The elastic moduli for nanoindentation have been plotted against the micro moduli of the selected set of polymers, shown in **Figure 2(a)**.

The other approaches like dynamic modulus approach are applied. This method is often termed as continuous stiffness measurement. The two important parameters in this are storage moduli and loss moduli [57]. The parameters can be also used with dynamic mechanical analysis (DMA). The storage moduli and loss moduli were obtained by both dynamic indentation and DMA for thermoplastic materials [58]. The results of the two methods were compared with each other as shown in **Figure 2(b)**. The consistent trend of greater dynamic indentation moduli than DMA moduli was observed for various materials. By this study, it can be observed that dynamic indentation moduli's can be subjected to a percent of error while characterizing the polymeric materials [59].

1.6 Nanoindentation in biological materials

The mechanical properties of biological materials are the early stage of development. Among all the techniques for mechanical characterization of biological

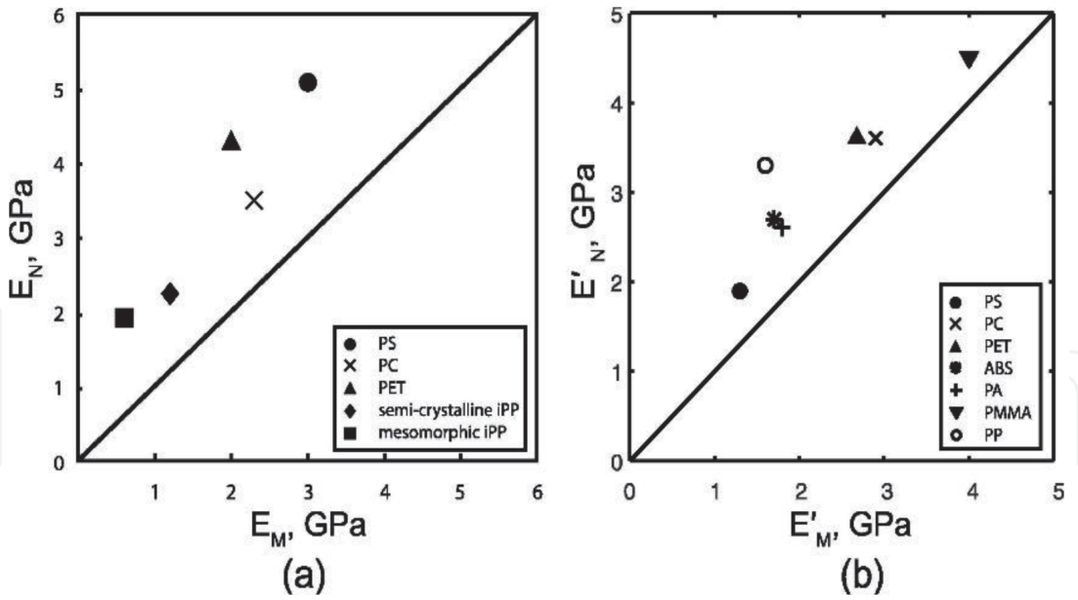

Figure 2.
(a) Surface nanoindentation and (b) cross-sectional nanoindentation [46].

materials, nanoindentation is most powerful tool due to its wide nanolevel force resolution [60] and mainly because of its surface and interfacial properties which play significant role not only in biology but also in synthesis of biomaterials. Therefore, the study of adoption of nanoindentation for biological materials and systems is of great interest.

New studies have been performed were it has been described how the diseases respond towards the mechanical characteristics up to the molecular level [61–66]. The method has also been used to carry out the mechanical analysis of fossils [67]. Indentation finds its application in describing the behavior of human skin which can be used to solve the aging problem of skin [68, 69]. Application of nanoindentation technique to biomaterials research is also expanded up to human enamel and eye tissues. In the coming years, the importance of nanoindentation testing in biology and biomaterials research is likely to show a rapid increase. Nanoindentation testing is implicated on both soft and hard tissues and also on biomaterials especially those with hierarchical microstructures. The nanoindentation methods are also applied to highlight the study of skeletal and dental tissues [70]. There also exist nanomechanics for soft, living tissues and polymeric biomaterials. Nanoindentation is now also being applied to the problem with studies examining connective tissues and polymers using both static and dynamic methods. The nanoindentation investigations on natural biomaterials have contributed significantly to biomimetics and the development of new composite materials. Continuing advancements in nanoindentation analysis will increase the method's utility in the characterization of biomaterials [71].

The measurement protocol for nanoindentation of biological samples (sometimes referred as bioindentation) takes into account the irregularity of the surface of the samples by incorporating an automatic surface detection procedure in the measurement matrix. The use of large spherical indenters facilitates contact detection on extremely soft samples (hydrogels [72], cartilage, scaffolds) by providing larger contact stiffness and averages surface and structural inhomogeneity. The penetrations seen in bioindentation are usually in the range of ten to several hundred micrometers, thus testing a large volume of tissue rather than single cells [73]. The applications of the bioindenter are very wide. Many human tissues are subject to mechanical loading and their mechanical characterization can provide valuable information for disease evolutions, treatments and also developments of artificial replacements (implants,

scaffolds). Bioindentation can be used in the diagnostic of disease (liver functions, arteries) and for fundamental research on treatment of these diseases [74].

2. Conclusion

Nanoindentation is a dynamic perceptible method for attaining mechanical properties from very limited content. In delicately regulated tests in which the acceptance of the elastic contact analysis are met, accuracy of a few percent is smoothly obtainable for indentations as micro as 10 nm. Specialists must be constantly aware of the holdings of variations from these suppositions on nanoindentation results. Exact evaluation for load, displacement and machine concurrence are requirement, as is an effective rational sketch of the shape of the tip, and a configuration devised to reduce the consequences of thermal drift and plasticity.

If there arise a need to measure a surface layer or other small volume, then evading the effects of surface conditions, or nearby free surfaces or interfaces, a practical indentation size range can be found analytically. Size effects, pile-up and anisotropy can advance precise deviations that must be alleged.

Nanoindentation is an area of powerful research and development and data analysis practices are frequently being revised. Future developments of nanoindentation are foreseen in the area of periodic incorporation of computer simulations, (FEM and others) and quantitative imaging technique to boost in analysis of depth-sensing indentation data, and much development in dynamic contact analysis system in addition to incorporation of acoustic practices.

Author details

Saquib Rouf[1]*, Sobura Altaf[1], Shezan Malik[1], Kaleem Ahmad Najar[2] and M.A. Shah[3]

1 SSM College of Engineering and Technology, Baramulla, India

2 Islamic University of Science and Technology, Awantipora, India

3 Department of Physics, National Institute of Technology-Srinagar, J&K, India

*Address all correspondence to: khansaquib626@gmail.com

References

[1] W.C Oliver, G.M Pharr (1992) An improved technique for determining hardness and elastic modulus using load and displacement sensing indentation experiments. Materials Research Innovation 7:1564.

[2] A. Tiwari, S. Natrajan (2017) Applied Nanoindentation in Advanced Materials. John Willey. ISBN: 978111908450.

[3] Anthony C, Fischer – Cripps (2011) Nanoindentation, Third Edition. Springer. ISBN: 978–1–4419-9871–2.

[4] Christopher A. Schuh (2006) Nanoindentation Studies of Materials. Materials Today 9(5): 32–40.

[5] Sagadevan S, Murugasen P (2014) Novel Analysis on the Influence of Tip Radius and Shape of the Nanoindenter on the Hardness of Materials. Procedia Materials Science (6): 1871–1878.

[6] G. Sundaranjan,M. Roy (2001) Hardness Testing. Encyclopedia of Materials: Science and Technology (Second Edition. PP: 3728–3736.

[7] T.H Pham, Q.M Phan and S.E Kim (2018) Identification of The Plastic Properties of Structural Steel Using Spherical Indentation. Materials Science and Engineering 711: 44–61.

[8] A. Lee, K. Komvopoulos (2018) Dynamic Spherical Indentation of Elastic- Plastic Solids. International Journal of Solids and Structures 146: 180–191.

[9] A.N. Masir, A. Darvizeh, A. zajkani (2019) Nanoindentation on Bio Inspired High Performance Nature Composite by Molecular Dynamic Method. Advanced Composites Letters 28:1–13.

[10] E. Broitman (2017) Indentation Hardness Measurement at Macro-, Micro-, and Nanoscale: A Critical Overview. Tribology Letters 65:23

[11] M.C. Aragon-Durate, A. Nevarez-Rascon, H.E. Esparza-Ponce, M. M. Nevarcz Rascon, R. P. Talamantes, C. Ornelas, J. Mendez-Nonell, J. Gonzalez-Hermandez, M. J. Yacaman, A. Hurtado-Macias (2017) Nanomechanical Properties of Zirconia-Yttria and Alumina Zirconia- Yttria Biomedical Ceramics, Subjected to Low Temperature Aging. Ceramics International 43(5):3931–3939

[12] I.N.Sneddon (1965) The Relation Between Load and Penetration in The Axisymmetric Boussineq Problem for a Punch of Arbitrary Profile. International Journal of Engineering Science 3(1):47–58.

[13] F. Doerner, D. S. Gardner, W. D. Nix (1986) Plastic Properties of Thin Films on Substrates as Measured by Submicron Indentation Hardness and Substrate Curvature Techniques. Journal of Materials Research 1(6): 845–851.

[14] H. Hertz (1881) On The Contact of Rigid Elastic Solids. J. Reine A19ngew. Math. 92, 1881, pp. 156–171.

[15] J. Cech, P. Hausild, O. Koravik, A. Materna (2016) Examination of Berkovich Indenter Tip Bluntness. Materials & Design 109: 347–357

[16] G.B. Ghorbal, A. Tricoteaux, A. Thuault, G. Louis, D. Chicot (2017) Comparison of Conventional Knoop and Vickers Hardness of Ceramic Materials. Journal of the European Ceramic Society37(6):2531–2535

[17] J. Gubicza, A. Juhasz, J. Lendvai (1996) A New Method for Hardness Determination from Depth Sensing Indentation Tests. Journal of Materials Research, 11(12):2964–2967.

[18] Y. Lu, Y. Su, W. Ge, T. Yang, Z. Yan, Y. Wang, S. Xia (2020) Conversion Between Vickers Hardness and Nanohardness by Correcting Projected Area with Sink-in and Pile-up Effects. Plasma Science and Technology 22 (06) 5602.

[19] M. Buijs, K. Korpel-Van Houten (1993) A Model for Lapping of Glass. Journal of Materials Science (28):3014–3020.

[20] G.R. Anstis, P. Chantikul, B. R lawn, D. B Marshall (1981) A Critical Evaluation of Indentation Techniques for Measuring Fracture Toughness: I, Direct Crack Measurements. Journal of the American Ceramic Society 64(9): 533–538.

[21] I. Hervas, A. Montagne, A. Van Gorp, M. Bentoumi, A. Thuault, A. Iost (2016) Fracture Toughness of Glasses and Hydroxyapatite: A Comparative Study of 7 Methods by Using Vickers Indenter. Ceramic International 42(11): 12740–12750

[22] J. Chevalier, L. Gremillard, S. Deville (2007) Low-Temperature Degradation of Zirconia and Implications for Biomedical Implants. Annual Review of Materials Research 37: 1–32.

[23] D. Coric, M. Majc Renjo, L. Curkovic (2017) Vicker Indentation Fracture Toughness of Y-TZP Dental Ceramics. International Journal of Refractory Metals and Hard Materials 64:14–19.

[24] M. Majic Renjo, L. Curkovic, S. Stefancic, D. Coric (2014) Indentation Size Effect of Y-TZP Dental Ceramics. Dental Materials 30(12):371–376.

[25] K. Niihara, R. Morena, D. P. H. Hasselman (1982) Evaluation of K Ic of Brittle Solids by the Indentation Method with Low Crack-to-Indent Ratios. Journal of Materials Science Letters 1(1): 13–16.

[26] D. Cesellas, M.M. Nagl, L. Llanes, M. Anglada (1996) Growth of Small Surface Indentation Cracks in Alumina and Zirconia Toughened Alumina. Key Engineering Materials 127–131:895–902.

[27] S. Palmqvist (1957) A Method to Determine The Fracture Toughness Brittle Materials, Especially Hard Metals. Jenkontorets Ann 141:303–307.

[28] S. Kaur, R.A. Cutler, D.K. Shetty (2009) Short-Crack Fracture Toughness of Silicon Carbide. Journal of the American Ceramic Society 92(1): 179–185.

[29] K. Niihara, R. Morena, D. P. H. Hasselman (1982) Evaluation of K Ic of Brittle Solids by the Indentation Method with Low Crack-to-Indent Ratios. Journal of Materials Science Letters 1(1): 13–16.

[30] A. Nastic, A. Merati, M. Bielawski, M. Bolduc, O. Fakolujo, M. Nganbe (2015) Instrumented and Vickers Indentation for the Characterization of Stiffness, Hardness and Toughness of Zirconia Toughened Al2O3 and SiC Armor. Journal of Material Science and Technology 31(8):773–783.

[31] S. J. Zinkle, W. C. Oliver (1986) Mechanical Property Measurements on Ion-Irradiated Copper and Cu-Zr. Journal of Nuclear Materials 141–143 (1): 548–552.

[32] K. Sato, H. Yamashita, A. Hirosako, S. Komazaki, Q. Xu, M. Onoue, R. Kasada, K. Yabuuchi, A. Kimura (2018) Investigation of Mechanical Properties of Stress- Relieved and Electron – Irradiated Tungsten after Hydrogen Charging. Nuclear Materials and Energy 17:29–33.

[33] B. Su, D.Y.W. Yu, H. Liang, G. Liu, Z. Huang, X. Liu, Z. Chen (2017) Damage Development of Sintered SiC Ceramics with the Depth Variation in Ar Ion-Irradiation at 600 °C. Journal of

European Ceramic Society 38(5): 2289–2296.

[34] Y. Chen, Y. Liu, E. G. Fu, C. Sun, K. Y. Yu, M. Song, J. Li, Y. Q. Wang, H. Wang, X. Zhang (2015) Usual Size – Dependent Mechanisms in Helium Ion – Irradiated Immiscible Coherent Cu/Co Nanolayers. Acta Materialia 84: 393–404.

[35] X. Xiao, L. Yu (2020) Nano-Indentation of Ion- Irradiated Nuclear Structural Materials: A Review. Nuclear Materials and Energy 22: 100721.

[36] Q.M. Wei, N. Li, *N. Mara*, M. Nastasi, A. Misra (2011) Suppression of Irradiation Hardening in Nanoscale V/Ag Multilayers. Acta Materialia 59(16): 6331–6340.

[37] P. Hosemann, J.G. Swadener, D. Kiener, G.S. Was, S. A Maloy, N.Li (2008) An Exploratory Study to Determine Applicability of Nano – Hardness and Micro – Compression Measurements for Yield Stress Estimation. Journal of Nuclear Materials 375(1): 135–143.

[38] I.J. Beyerlein, M.J. Demkowicz, A. Misra, B.P. Uberuaga (2015) Defect – Interface Interactions. Progress in Materials Science 74:125–210.

[39] X. Zhang, K. Hattar, Y. Chen, L. Shao, J. Li, C. Sun, K. Yu, Nan Li, M. L. Taheri, H. Wang, J. Wang, M. Nastasi (2018) Radiation Damage in Nanostructured Materials 92: 217–321.

[40] C. Shin, H. Jin, M. Kim (2009) Evaluation of the Depth-Dependent Yield Strength of a Nanoindentation Ion – Irradiated Fe-Cr Model Alloy by Using a Finite Element Modeling. Journal of Nuclear Materials 392(3): 476–481.

[41] D.E.J. Armstrong, C.D. Hardie, J.S. K.L. Gibson, A.J. Bushby, P.D. Edmondson, S.G. Roberts (2015) Small – Scale Characterisation of Irradiated Nuclear Material: Part II Nanoindentation and Micro- Cantilever Testing of Ion Irradiated Nuclear Materials 462: 374–381.

[42] J. A. Sharon, K. Hattar, B.L. Boyce, L.N. Brewer (2013) Compressive Properties of <110> Cu Micro-Pillars after High – Dose Self-Ion Irradiation. Materials Research Letters 2(2): 57–62.

[43] T. Wei, A. Xu, H. Zhu, M. Lonescu, D. Bhattacharyya (2017) In Situ Micro-Compression Testing of He^{2+} Ion Irradiated Titanium Aluminide. Nuclear Instruments and Methods in Physics Research Section B: Beam Interactions with Materials and Atoms 409: 288–292.

[44] M. Saleh, A. Xu, C. Hurt, M. Lonescu, J. Daniels, P. Munroe, L. Edwards, D. Bhattacharyya (2019) Oblique Cross - Section Nano Indentation for Determining the Hardness Change in Ion- Irradiated Steel. International Journal of Plasticity 112: 242–256.

[45] N. K. Mukhopadhyay, P. Paufler (2013) Micro- and Nanoindentation Techniques for Mechanical Characterisation of Materials. International Materials Reviews 51 (4): 2019–245.

[46] D. Kiener, A.M. Minor, O. Anderoglu, Y. Wang (2012) Application of Small – Scale Testing for Investigation of Ion – Beam -Irradiated Materials. Journal of Materials Research 27(21):2724–2736.

[47] J. Weaver, C. Sun, Y. Wang, S.R. Kalidindi, R.P. Doerner, N.A. Mara, S. Pathak (2018) Quantifying the Mechanical Effects of He, W and He+W Ion Irradiation on Tungsten with Spherical Nanoindentation. Journal of Material Science 53: 5296–5316.

[48] S. Pathak, S.R. Kalidindi, J.S. Weaver, Y. Wang, R.P. Doerner, N.A. Mara (2017) Probing Nanoscale Damage

Gradients in Ion-Irradiated Metals Using Spherical Nanoindentation 7: 11918.

[49] Q. Dong, H. Qin, Z. Yao, M.R. Daymond (2019) Irradiation Damage and Hardening in Pure Zr and Zr-Nb Alloys at 573 K from Self-Ion Irradiation. Materials & Design 161: 147–159.

[50] H. Hardiman, T.J. Vaughan, C.T. McCarthy (2017) A Review of Key Developments and Pertinent Issues in Nanoindentation Testing of Fibre Reinforced Plastic Microstructures. Composite Structures 180:782–792.

[51] D. Tranchida, S. Piccarolo, J. Loos, A. Alexeev (2006) Accurately evaluating Young's modulus of polymers through nano indentations: A phenomenological correction factor to the Oliver and Pharr procedure. Applied Physics Letters 89: 171905.

[52] D. Tranchida, S. Piccarolo, J. Loos, A. Alexeev (2007) Mechanical Characterization of Polymers on a Nanometer Scale through Nano indentation. A Study on Pile - up and Viscoelasticity. Macromolecules 40: 1259–1267.

[53] M. R. Vanlandingham, J. S. Villarrubia, W. F. Guthrie, G. F. Meyers (2001) Nanoindentation of Polymers: An Overview. Macromolecular Symposia 167(1):15–44.

[54] J. Deuschle (2008) Mechanics of soft polymer identification. Universitat Stuttgart: http://dx.doi.org/ 10.18419 / opus-907

[55] J. M. Kranenburg, C.A. Tweedie, K. J. V. Vliet, U. S. Schubert (2009) Challenges and Progress in High-Throughput Screening of Polymer Mechanical Properties by Indentation. Advanced Materials 21(35):3551–3561.

[56] H. Lu, B. Wang, J. Ma, G. Huang, H. Viswanathan (2003) Measurement of Creep Compliance of Solid Polymers by Nanoindentation. Mechanics of Time-Dependent Materials 7: 189–207.

[57] G. M. Odegard, T.S. Gates, H. M. Herring (2005) Characterization of Viscoelastic Properties of Polymeric Materials Through Nanoindentation. Experimental Mechanics 45: 130–136.

[58] P. Frontini, S. Lotfian, M. A. Monclus, J. M. Aldareguia (2015) High Temperature Nanoindentation Response of RTM6 Epoxy Resin at Different Strain Rates. Experimental Mechanics 55(5):1–12.

[59] J. Giro-Paloma, J. J. Roa, A. M. Diez-Pascual, E. Rayon, *A. Flores*, M. Martínez, J. M. Chimenos, A.I. Fernandez (2013) Depth-Sensing Indentation Applied to Polymers: A Comparison Between Standard Methods of Analysis in Relation to the Nature of the Materials. European Polymer Journal 49(12): 4047–4053.

[60] N. E. Kurland, Z. Drira, V. K. Yadavalli (2012) Measurement of Nanomechanical Properties of Biomolecules Using Atomic Force Microscopy. Micron 43 (2–3): 116–128.

[61] S. Gracia-Manyes, O. Domenech, F. Sanz, M. T. Montero, J. Harnandez-Borrell (2007) Atomic Force Microscopy and Force Spectroscopy Study of Langmuir–Blodgett Films Formed by Heteroacid Phospholipids of Biological Interest. Biochimica et Biophysica Acta (BBA) – Biomembranes 1768(5):1190–1198.

[62] S. Huang, D. E. Ingber (2005) Cell Tension, Matrix Mechanics, and Cancer Development. Cell Cancer 8(3):175–176.

[63] D. E. Discher, P. Janmey, Y. Wamg (2005) Tissue Cells Feel and Respond to the Stiffness of Their Substrate. Science 310(5751): 1139–1143.

[64] A. J. Engler, S. Sen, H. L. Sweeney, D. E. Discher (2006) Matrix Elasticity

Directs Stem Cell Lineage Specification. Cell 126 (4): 677–689.

[65] M. Stolz, R. Gottardi, R. Raiteri, S. Miot, I. Martin, R. Imer, U. Staufer, A. Randucanu, M. Duggelin, W. Baschong, A.U. Daniels, N. F. Friederich, A. Aszodi, U. Aebi (2009) Early Detection of Aging Cartilage and Osteoarthritis in Mice and Patient Samples Using Atomic Force Microscopy. Nature Nanotechnology 4:186–192.

[66] R. J. H. Cloots, J. A. W. van Dommelen, S. Kleiven, M. G. D. Geers (2012) Multi-scale Mechanics of Traumatic Brain Injury: Predicting Axonal Strains from Head Loads. Biomechanics and Modeling in Mechanobiology (12): 137–150.

[67] S. E. Olesiak, M. Sponheimer, J. J. Eberle, M. L. Oyen, V. L. Ferguson (2010) Nanomechanical Properties of Modern and Fossil Bone. Palaeogeography, Palaeoclimatology, Palaeoecology 289 (1–4): 25–32.

[68] H. Oxlund, J. Manschot, A. Viidik (1988) The Role of Elastin in the Mechanical Properties of Skin. Journal of Biomechanics 21(3): 213–218.

[69] A. Agache, P. Humbert (2004) Measuring the Skin. Springer-Verlag Berlin Heidelberg. ISBN: 978–3–642-05691-8.

[70] K. Subramani, W. Ahmed (2017) Emerging Nanotechnologies in Dentistry-2nd Edition. Micro & Nanotechnologies Series Elsevier, ISBN: 978–0–12-812291-4.

[71] A.B. Mann (2005) Nanoindentation - Surfaces and Interfaces for Biomaterials, Editor(s): P. Vadgama. Woodhead Publishing Series in Biomaterials (225–247). ISBN: 978–1–855-73930-7.

[72] Y. Hu, J. You, D. Auguste, Z. Suo, J. Vlassak (2012) Indentation: A simple, Non-destructive Method for Characterizing the Mechanical and Transport Properties of pH-Sensitive Hydrogels. Journal of Materials Research 27(1): 152–160.

[73] C. Cai, Q. Yu, W. Li, J. Zheng, Z. Zhou (2017) Experimental Creep Behavior of Porcine Liver under Indentation with Laparoscopic Grasper for MIS Applications. Biosurface and Biotribology 3(2): 56–65.

[74] J. Nohava, M. Swain, P. Eberwein (2014) Micromechanical Properties of Polyacrylamide Hydrogels Measured by Spherical Nanoindentation. Key Engineering Materials 606: 121–124.